Biochemical and Biophysical Research Communications 424 (2012) 530–537

Contents lists available at SciVerse ScienceDirect

Biochemical and Biophysical Research Communications

journal homepage: www.elsevier.com/locate/ybbrc

Reactive oxygen species-mediated activation of JNK and down-regulation of DAXX are critically involved in penta-O-galloyl-beta-D-glucose-induced apoptosis in chronic myeloid leukemia K562 cells

Tae-Rin Kwon [a,1], Soo-Jin Jeong [a,1], Hyo-Jeong Lee [a], Hyo-Jung Lee [a], Eun Jung Sohn [a], Ji Hoon Jung [a], Ji-Hyun Kim [a], Deok-Beom Jung [a], Junxaun Lu [b], Sung-Hoon Kim [a,*]

[a] College of Oriental Medicine, Kyung Hee University, Seoul 130-701, Republic of Korea
[b] The Hormel Institute, University of Minnesota, Austin, MN 55912, USA

ARTICLE INFO

Article history:
Received 11 June 2012
Available online 6 July 2012

Keywords:
Chronic myeloid leukemia
Apoptosis
JNK
Reactive oxygen species
PGG

ABSTRACT

Although 1,2,3,4,6-penta-O-galloyl-beta-D-glucose (PGG) was well known to have antitumor activities in breast, prostate, kidney, liver cancers and HL-60 leukemia via regulation of caspase 3, p53, S-phase kinase-associated protein 2 (Skp2) and insulin receptor signaling, the underlying mechanism of PGG-induced apoptosis linked with reactive oxygen species (ROS) mediated c-Jun N-terminal kinase (JNK) and DAXX was never elucidated in chronic myeloid leukemia (CML) K562 cells until now. Herein PGG significantly decreased the viability of CML cell lines such as K562 and KBM-5 without hurting normal peripheral blood lymphocytes (PBLs). PGG increased the number of TUNEL-positive cells and the sub-G1 cell population as well as activated caspase cascades including caspase-8, -9 and -3 in K562 cells. Interestingly, a significant activation of JNK by PGG was observed by MULTIPLEX assay and Western blotting. Conversely, JNK inhibitor D-JNKi suppressed the cleavages of caspase 3 and PARP induced by PGG in K562 cells. Also, PGG dramatically enhanced generation of ROS and reduced the expression of death-domain-associated protein (DAXX). Of note, ROS inhibitor acetyl-L-cysteine (NAC) reversed JNK-dependent apoptosis and DAXX inhibition induced by PGG. Overall, these findings suggest that ROS-dependent JNK activation and DAXX downregulation are critically involved in PGG-induced apoptosis in K562 cells.

1. Introduction

Chronic myelogenous leukemia (CML) is a myeloproliferative disorder characterized by a triphasic course typically beginning as an indolent chronic phase and progressing to accelerated phase and then to blast crisis. At a cytogenetic and molecular level, most patients with CML demonstrate *BCR-ABL* fusion genes in hematopoietic progenitor cells, with a reciprocal translocation between chromosomes 9 and 22 leading to a shortened chromosome 22, called the Philadelphia chromosome [1,2]. 1,2,3,4,6-Penta-O-galloyl-beta-D-glucose (PGG) has multi-biological activities such as anti-proliferative, anti-angiogenic, apoptotic and anti-diabetic activities [3]. Also, PGG, a naturally occurring gallotannin polyphenolic compound from *Rhus chinensis* MILL, showed antitumor activities against various types of cancer cells, including prostate [4], lung [5], breast [6], melanoma [7], liver cancers [8] and sarcomas [9]. However, the underlying mechanism of PGG-induced apoptosis in hematologic malignancies still remains unclear. The Fas death domain-associated protein (DAXX) is known as a Fas binding protein. DAXX promotes the apoptosis through activation of c-JNK-N terminal kinase (JNK) pathway dependent on Fas associated death domain protein [10]. Thus, in the present study, the molecular mechanisms responsible for anti-cancer activity of PGG through apoptosis induction in K562 cells were elucidated in association with ROS dependent JNK and DAXX signaling.

2. Materials and methods

2.1. Isolation of PGG

PGG was isolated from the gallnut of *Rhus chinensis* MILL as previously described [11]. The yellowish active compound was identified as PGG by NMR and FAB–MS analysis. The purity of PGG was estimated to be >96% by high performance liquid chromatography (HPLC).

* Corresponding author. Address: Cancer Preventive Material Development Research Center, College of Oriental Medicine, Kyung Hee University, 1 Hoegi-dong, Dongdaemun-gu, Seoul 131-701, South Korea. Fax: +82 2 964 1064.
E-mail address: sungkim7@khu.ac.kr (S.-H. Kim).
[1] These authors contributed equally to this work.

0006-291X/$ - see front matter © 2012 Elsevier Inc. All rights reserved.
http://dx.doi.org/10.1016/j.bbrc.2012.06.150

2.2. Cell culture

K562 (CML), HL-60 (acute myeloid leukemia) and U937 (histiocytic leukemia) cells were purchased from American Type Culture Collection (ATCC) (Rockville, MD). The cells were maintained in RPMI 1640 containing 10% fetal bovine serum (FBS). KBM-5 (CML) cells were kindly provided by Dr. Bharat B. Aggarwal (The University of Texas M.D. Anderson Cancer Center, Houston, TX) and maintained in IMDM culture medium supplemented with 15% FBS.

2.3. Human peripheral blood lymphocytes (PBLs) isolation

PBLs were isolated from human blood samples of healthy donor by Ficoll-Hypaque (GE Healthcare, Uppsala, Sweden) gradient centrifugation.

2.4. Cytotoxicity assay

Cytotoxic effect of PGG was determined by sodium 2,3-bis(2-methoxy-4-nitro-5-sulfophenyl)-2H-tetrazolium-5-carboxanilide inner salt (XTT) assay. Cells (2×10^4 cells/100 μl/well) were seeded on 96-well microplates, treated with various concentrations of PGG (0, 10, 20, 40 or 80 μM) for 24 h and incubated with XTT labeling mixture (125 μM XTT/25 μM PMS (phenazine methosulphate)) at 37 °C for 2 h. Optical density (OD) was measured using a microplate reader (Molecular Devices Co., Sunnyvale, CA) at 450 nm. Cell viability was calculated as a percentage of viable cells in PGG-treated group compared with untreated control by following equation. Cell viability (%) = [OD (PGG) − OD (Blank)]/[OD (Control) − OD (Blank)] × 100

2.5. TUNEL assay

TUNEL assay was performed by using Dead End™ fluorometric TUNEL assay kit (Promega, Madison, WI) according to the manufacturer's instructions. Cells were seeded on poly-L-lysine coated coverslips and fixed in 4% paraformaldehyde for 30 min followed by permeabilization with 0.2% Triton X-100. The cells were then incubated with nucleotide mix and terminal deoxynucleotidyl transferase (TdT) enzyme for 1 h at 37 °C in dark and terminated by 2 × SSC for 15 min at room temperature. The slides were mounted with mounting medium containing 4′,6-diamidino-2-phenylindole (DAPI) (VECTOR, Burlingame, CA, USA) and apoptotic nuclei were visualized under Axio vision 4.0 fluorescence microscope (Carl Zeiss Inc., Weimar, Germany)

2.6. Cell cycle analysis

Cells were fixed in 70% chilled ethanol at −20 °C, incubated with RNase A (0.1 mg/ml in PBS) at 37 °C for 1 h and stained with propidium iodide (PI) (50 μg/ml) for 30 min at room temperature in dark. After filtering the cells with nylon mesh (40 μm), the stained cells were analyzed for DNA content by FACSCalibur (Becton Dickinson, Franklin Lakes, NJ) using Cell Quest program (Becton Dickinson, Franklin Lakes, NJ).

2.7. Western blotting

Western blotting was performed as previously described [12]. Whole cell extracts were prepared using cell lysis buffer (50 mM Tris–HCl, pH 8.0, 150 mM NaCl, 1 mM EDTA, 1% NP-40, 0.25% deoxycholate acid) containing protease inhibitor cocktail (Roche Applied Science, Inndianapolis, IN). Protein samples were quantified by using Bio-Rad DC protein assay kit II (Bio-Rad, Hercules, CA), separated onto 8–15% SDS–PAGE gels and electrotransferred to a nitrocellulose membranes. After blocking with 5% nonfat skim milk, the blots were probed with antibodies against cleaved caspase-3, cleaved caspase-8, caspase-9, phospho-JNK, JNK (Cell Signaling Tech., Danvers, MA), DAXX, Bcl-2, Mcl-1_L, Survivin, PARP (Santa Cruz Biotechnology, Santa Cruz, CA), and β-actin (Sigma, St. Louis, MO), and exposed to horseradish peroxidase (HRP)-conjugated anti-mouse or rabbit secondary antibodies. Protein expression was detected by using enhanced chemiluminescence (ECL) system (Amersham Pharmacia, Piscataway, NJ).

2.8. Caspase-3 activity assay

Caspase-3 activity was evaluated by measuring proteolytic cleavage of chromogenic substrate by using the colorimetric caspase-3 assay kit (R&D Systems, Minneapolis, MN) following the manufacturer's instruction. Cells were lysed using lysis buffer (100 mM HEPES, pH 7.4, 140 mM NaCl, 1% protease inhibitor cocktail) and centrifuged at 13,000*g* at 4 °C for 10 min. Supernatant was incubated with 200 μM DEVD-pNA or IETD-pNA, and 5 mM dithiothreitol (DTT) at 37 °C for 2 h. The absorbance of enzymatically released pNA was measured a microplate reader (Molecular Devices Co., Sunnyvale, CA) at 405 nm.

2.9. Bioplex analysis

The MILLIPLEX™ MAP 8-plex multi-pathway signaling kit (Millipore, Billerica, MA) was used to detect changes in the phosphoylation of signaling proteins extracellular signal-regulated kinase (ERK)/ mitogen activated protein kinase (MAPK) 1/2 (Thr^{185}/Tyr^{187}), signal transducers and activators of transcription 3 (STAT3) (Ser^{727}), c-Jun N-terminal kinase (JNK) (Thr^{183}/Tyr^{185}), p70 S6 kinase (Thr^{412}), IκBα (Ser^{32}), STAT5a/b ($Tyr^{694/699}$), cAMP response element-binding (CREB) (Ser^{133}), and p38 MAPK ($Thr^{180/Tyr182}$). Cell lysates were incubated with anti-phospho protein beads for 2 h at room temperature followed by detection antibody and streptavidin-PE (SAPE) incubation for 15 min at room temperature in MILLIPLEX MAP 96-well filter plate. The plate was analyzed on the Luminex® system. All samples were analyzed twice, in triplicate.

2.10. Measurement of reactive oxygen species (ROS) production

Level of ROS was measured as previously described [13]. In brief, cells were stained with 2.5 μM DCFDA at 37 °C for 30 min and the fluorescence intensity was analyzed by FACSCalibur (Becton Dickinson, Franklin Lakes, NJ) using Cell Quest Software (BD Bio-sciences, San Jose, CA).

2.11. Immunofluorescence assay

Cells were fixed with 4% paraformaldehyde (PFA) and blocked in 0.1% Triton X-100/5% BSA in PBS for 25 min at 4 °C, and incubated with anti-DAXX (Santa Cruz Biotechnology, Santa Cruz, CA) for 1 h at room temperature. Then, anti-rabbit IgG (1:1000) fluorescein isothiocyanate (FITC)-conjugate (Abcam, Cambridge, UK) was used as a secondary antibody for 1 h at room temperature. The immunostained cells were mounted with medium containing DAPI and visualized by use of Olympus FLUOVIEW FV10i confocal microscope.

2.12. Statistical analysis

Data were presented as means ± standard deviation (SD) of a minimum of 3 or more replicates. The statistically significant differences between control and PGG-treated groups were calculated by Student's *t*-test using Sigmaplot software (Systat Software Inc., San Jose, CA).

3. Results

3.1. PGG exerts the cytotoxicity against chronic myeloid leukemia cell lines

The cytotoxic effect of PGG was evaluated by XTT assay. Chronic myeloid leukemia cell lines K562 and KBM-5, and normal peripheral blood lymphocytes (PBLs) were treated with various concentrations of PGG (0, 10, 20, 40 or 80 μM) for 24 h. As shown in Fig. 1A, PGG significantly reduced the viability of K562 and KBM-5 cells in a dose-dependent manner. In contrast, PGG did not influence the viability of normal PBLs. To examine whether the cytotoxicity of PGG in CML cells was associated with apoptosis, cell cycle analysis was performed to determine sub-G1 DNA contents undergoing apoptosis. PGG treatment mediated the accumulation of K562 cells at sub-G1 phase in a dose-dependent manner (Fig. 1B). The sub-G1 contents were increased from 1.61 ± 0.33% to 16.31 ± 4.77% at 80 μM. Consistent with the results of cell cycle analysis, TUNEL assay revealed that PGG increased the number of FITC-stained TUNEL positive cells showing DNA fragmentation (Fig. 1C). In addition, inverted microscopic observation exhibited apoptotic morphological features such as cell shrinkage (arrows) in PGG-treated K562 cells (Fig. 1D).

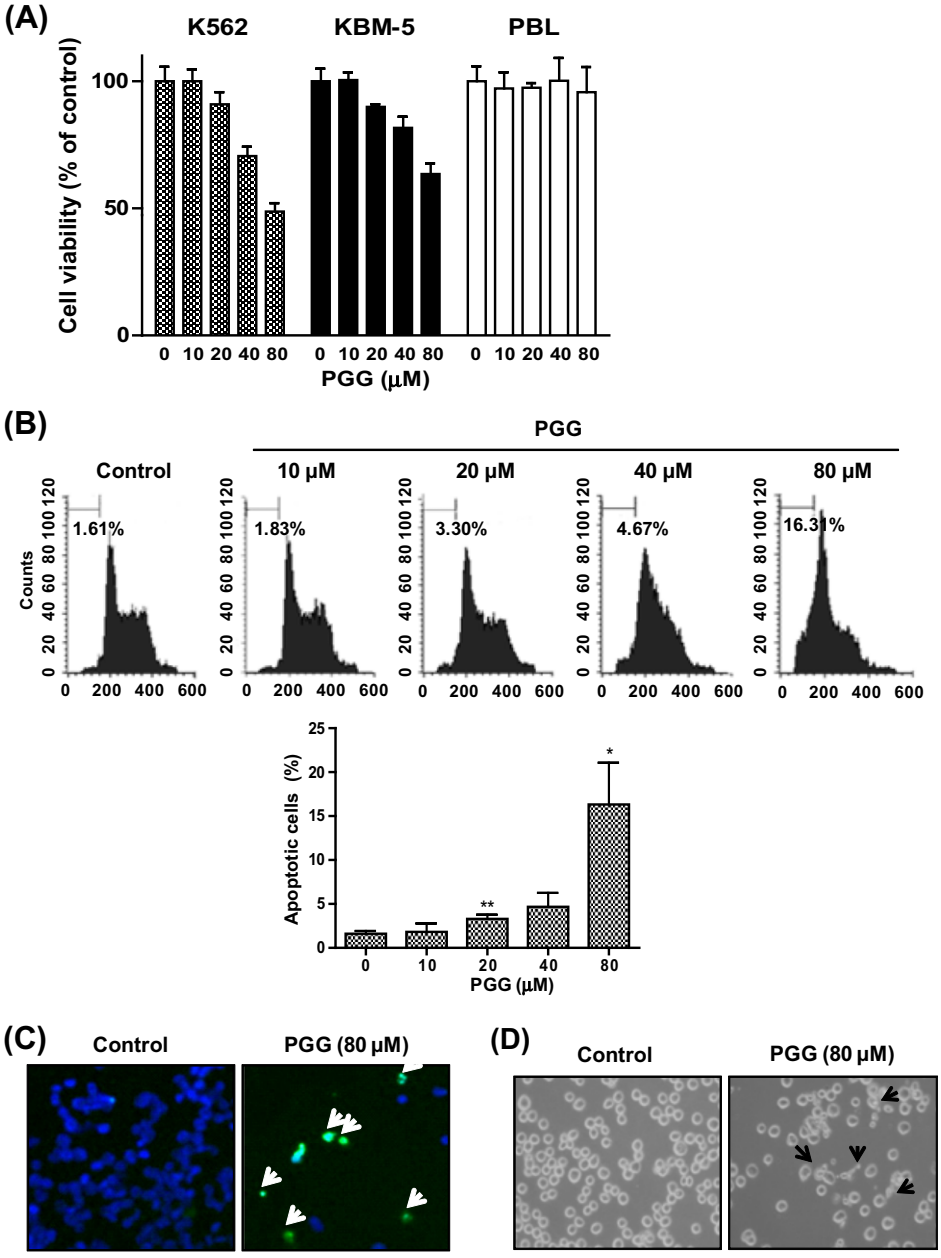

Fig. 1. PGG induces apoptotic cell death in K562 cells. (A) Chronic myeloid leukemia cell lines K562 and KBM-5, and normal peripheral blood lymphocytes (PBLs) were treated with various concentrations of PGG (0, 10, 20, 40 or 80 μM) for 24 h. XTT assay was performed to measure the cytotoxicity of PGG. (B) K562 cells were treated with various concentrations of PGG (0, 10, 20, 40 or 80 μM) for 24 h. After fixing in 75% ethanol, cells were stained with propidium iodide (PI) and cell cycle was analyzed by flow cytometry. Graphs represent the percentages of sub-G1 DNA contents. Data are presented as means ± SD. $^{*}p < 0.05$ and $^{**}p < 0.01$ *vs.* untreated control. (C) and (D) K562 cells were treated with or without PGG (80 μM) for 24 h. (C) TUNEL staining was performed to detect DNA fragmentation. The stained cells were visualized under Axio vision 4.0 fluorescence microscope at 630× of original magnification. DAPI was utilized as a counter staining. (D) Cell morphological changes were observed under an inverted microscopy at 200× of original magnification.

3.2. PGG induces apoptosis through the intrinsic pathways in K562 cells

Apoptosis can be controlled by intrinsic and/or extrinsic pathways [14]. In the present study, we observed that PGG dramatically increased the cleavages of caspase-8, -9 and -3 as well as PARP (caspase-3 substrate) in a dose- and time-dependent manner (Fig. 2A and B). The significance of caspase activation in PGG-induced apoptosis was confirmed using several caspase inhibitors including z-VAD-fmk (pan caspase inhibitor), z-DEVD-fmk (caspase-3 inhibitor), z-IETD-fmk (caspase-8 inhibitor), and z-LEHD-fmk (caspase-9 inhibitor). Pretreatment of z-VAD-fmk clearly blocked the PARP cleavage by PGG treatment (Fig. 2C, compare lanes 2 and 3). z-DEVD-fmk and z-LEHD-fmk, but not z-IETD-fmk, partially reduced the level of PARP cleavage in PGG-treated K562 cells (Fig. 2C). Consistently, PGG did not activate caspase-3 in the presence of z-VAD-fmk (Fig. 2D). Furthermore, PGG attenuated the expressions of anti-apoptotic Mcl-1_L, Bcl-2 and Survivin in a dose- and time-dependent manner (Fig. 2E and F), suggesting PGG induces apoptosis through the intrinsic pathway. Interestingly, the inhibitory effect of PGG on Mcl-1_L was observed in CML cell line KBM-5, but not in acute myeloid leukemia (AML) cells HL-60 and U937 (Fig. 2G).

3.3. JNK plays an important role in PGG-induced apoptosis in K562 cells

To delineate the molecular mechanisms involved in PGG-induced apoptosis in K562 cells, we performed bioplex analysis by using MULTIPLEX Map 8-plex Multipathway signaling kit. The

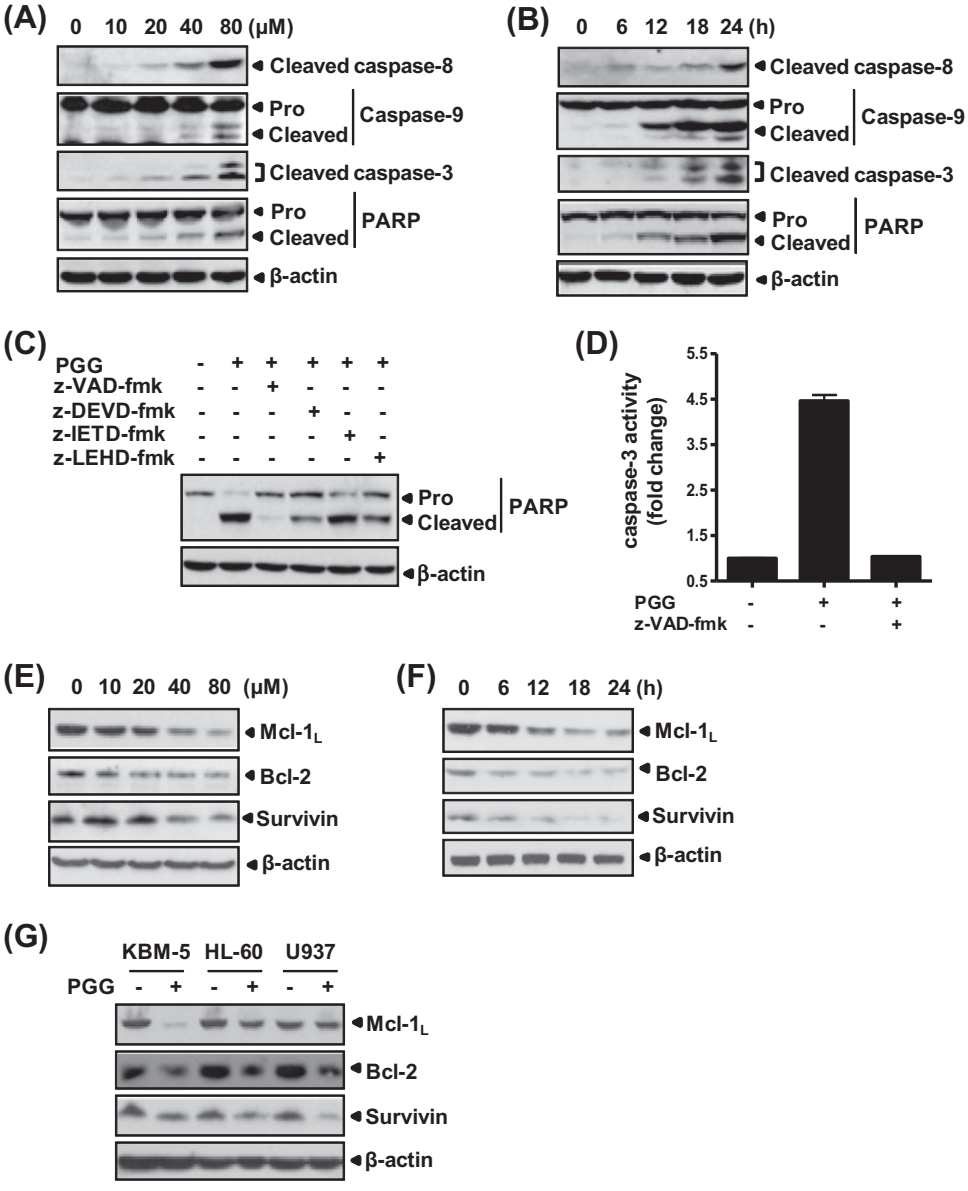

Fig. 2. PGG activates caspase cascade and regulates apoptosis-related protein expressions in K562 cells. (A) Cells were treated with various concentrations of PGG (0, 10, 20, 40 or 80 μM) for 24 h. (B) Cells were treated with PGG (80 μM) for 0, 6, 12, 18 or 24 h. Cell lysates were prepared and subjected to Western blotting for cleaved caspase-8, -9 and -3, and PARP. (C) and (D) After pretreatment with caspase inhibitors (50 μM) for 1 h, cells were treated with PGG (80 μM) for 24 h. (C) Western blotting was performed with anti-PARP antibody. (D) Caspase-3 activity was measured by using Fluorigenic caspase-3 iuminometric assay kit. (E) Cells were treated with various concentrations of PGG (0, 10, 20, 40 or 80 μM) for 24 h. (F) Cells were treated with PGG (80 μM) for 0, 6, 12, 18 or 24 h. (G) KBM-5 (chronic myeloid leukemia), HL-60 (acute myeloid leukemia) and U937 (histiocytic leukemia) were treated with or without 40 μM) for 24 h. Western blotting was performed to determine the expression of anti-apoptotic Mcl-1_L, Bcl-2, Bax and Survivin.

phosphorylation status of eight different phospho-proteins including ERK, STAT3, JNK, p70S6 K, IκBα, STAT5a/b, CREB and p38 MAPK were measured in cells treated with PGG (0, 40 or 80 μM). As shown in Fig. 3A, PGG treatment dramatically enhanced level of JNK phosphorylation in a dose-dependent manner. Consistent with the results of bioplex analysis, PGG remarkably increased phosphorylation of JNK in a dose- and time-dependent manner (Fig. 3B and C). Of note, we found a significant increase of phospho-JNK in PGG-treated KBM-5 cells, but not in HL-60 and U937 (Fig. 3D).

To explore whether activation of JNK is involved in the PGG-induced apoptosis pathway, a specific inhibitor for JNK (D-JNKi) was added with or without PGG. Pretreatment of JNK inhibitor clearly blocked caspase-3 activation and PARP cleavage (Fig. 3E). Consistently, JNK inhibitor, but not p38 (SB203580) and ERK (PD98059) inhibitors, blocked PGG induced caspase-3 activation (Fig. 3F) and apoptotic cells (Fig. 3G) in KBM-5 cells. Taken together, these results indicate that JNK activation plays a crucial role in PGG-induced apoptosis pathway in K562 cells.

3.4. PGG induces apoptosis via activation of the ROS/DAXX/JNK signaling in K562 cells

Reactive oxygen species (ROS) is an important group of free radicals that are capable of eliciting direct damaging effects or acting as critical intermediate signaling molecules, leading to oxidative stress and a series of biological consequences include apoptosis and also one of the main factors of JNK activation [15]. Thus, we measured the level of ROS generation using DCFDA in K562 cells treated with PGG. As show in Fig. 4A, exposure of cells to PGG slightly increased ROS production at 1 h (6.14 ± 2.03%), while significantly enhancing at 24 h (18.56 ± 0.26%) compared with untreated control (1.08 ± 0.19%). In contrast, co-treatment of PGG with ROS inhibitor N-acetyl cysteine (NAC) completely impeded PGG-mediated ROS generation in K562 cells (Fig. 4A).

Recently, Khelifi et al. suggested that DAXX is a protein required for stress-induced cell death and JNK activation [16]. In this regard, the effect of PGG on expression of DAXX protein was analyzed in K562 cells. We observed that PGG suppressed

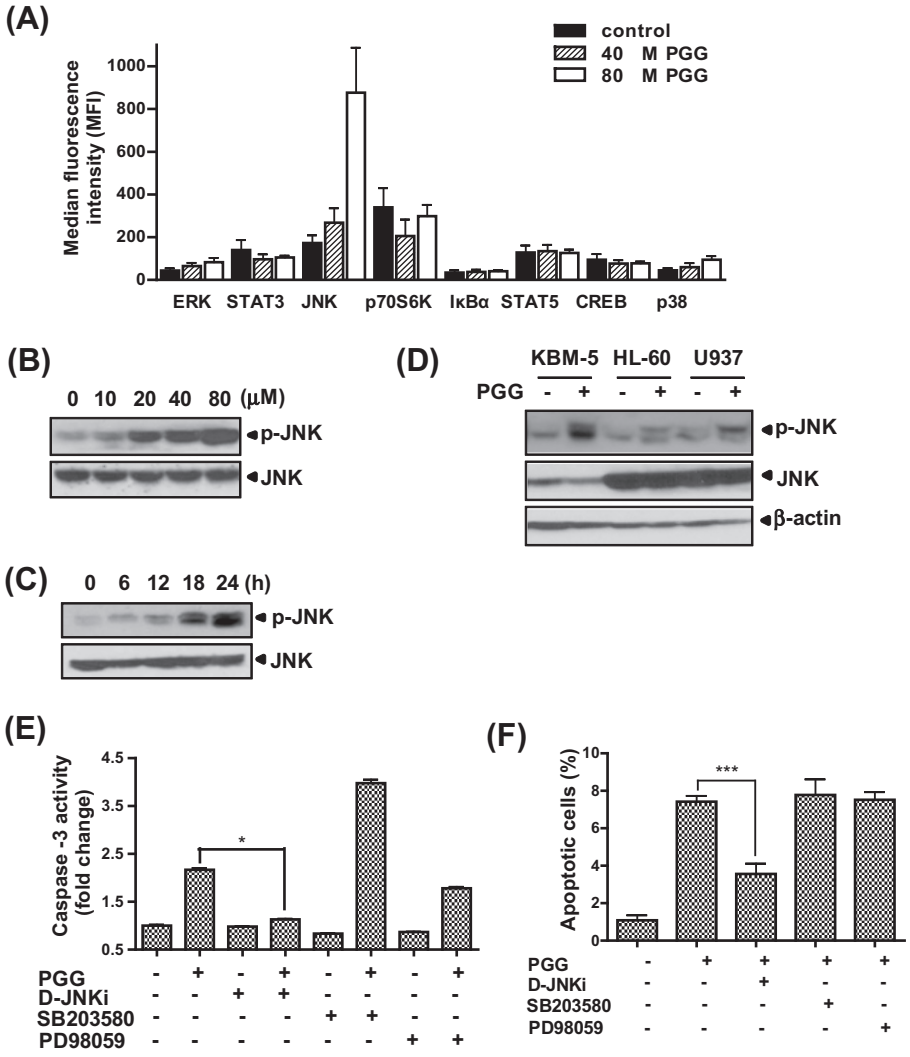

Fig. 3. PGG induces apoptosis via activation of JNK in K562 cells. (A) Cells were treated with PGG (0, 40 or 80 μM) for 24 h. Multiplex microbead immunoassay was performed to evaluate effect of PGG on the phosphorylation status of eight signaling proteins by using MULTIPLEX Map 8-plex assay signaling kit. (B) Cells were treated with various concentrations of PGG (0, 10, 20, 40 or 80 μM) for 24 h. (C) Cells were treated with PGG (80 μM) for 0, 6, 12, 18 or 24 h. (D) KBM-5, HL-60 and U937 were treated with or without PGG (40 μM) for 24 h. Western blotting was performed for phospho-JNK and JNK. (E–G) Cells were pre-treated with MAPK inhibitors [D-JNK-i inhibitor (30 μM), SB203580 (10 μM) or PD98059 (25 μM)] for 1 h, and then exposed to PGG (80 μM) for 24 h. (E) Caspase-3 activity was measured by using fluorigenic caspase-3 luminometric assay kit. (F) Sub G1 population was analyzed by cell cycle analysis. Data are presented as means ± SD. $^{*}p < 0.05$ and $^{***}p < 0.001$ *vs.* PGG-treated group.

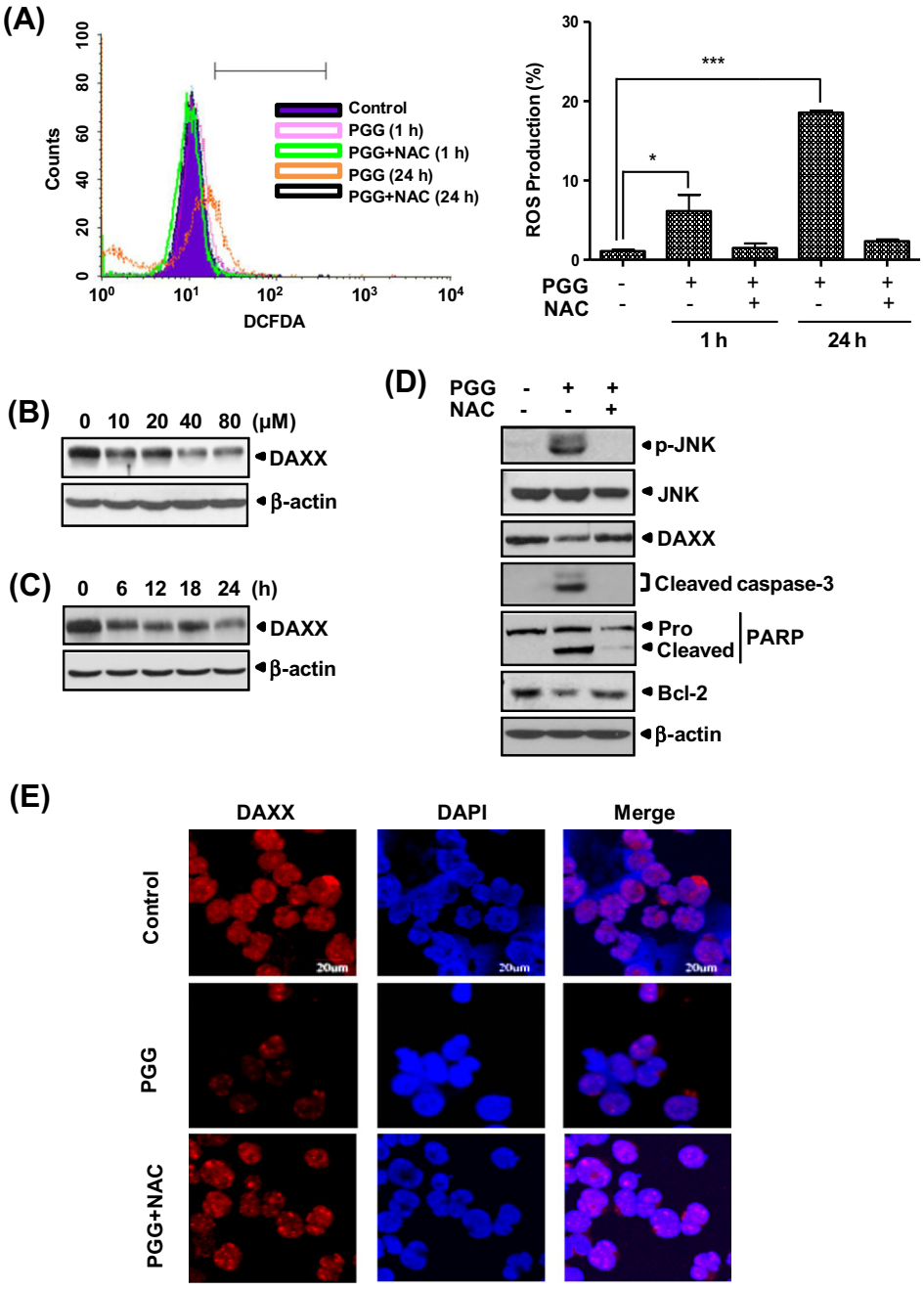

Fig. 4. Reactive oxygen species (ROS)-mediated signaling is involved in PGG-induced apoptosis in K562 cells. (A) Cells were incubated with or without PGG (80 μM) in the absence or presence of the free radical scavenger NAC (20 mM) for 1 or 24 h. ROS levels were analyzed using oxidation sensitive fluorescent dye (H_2-DCFDA) by flow cytometric analysis. Graphs represent the percentages of ROS generation. Data are presented as means ± SD. $^{*}p < 0.05$ and $^{***}p < 0.001$ *vs.* untreated control. (B) Cells were treated with various concentrations of PGG (0, 10, 20, 40 or 80 μM) for 24 h. (C) Cells were treated with PGG (80 μM) for 0, 6, 12, 18 or 24 h. Cell lysates were prepared and subjected to Western blotting to determine the expression of DAXX. (D and E) After preincubation with NAC for 1 h, cells were treated with PGG (80 μM) for 24 h. (D) Western blotting was performed for phospho-JNK, JNK, DAXX, PARP, cleaved caspase-3 and Bcl-2. (E) Immunocytochemical staining was carried out anti-DAXX antibody. Cells were counterstained with DAPI prior to mounting. The stained cells were visualized by the use of Olympus FLUOVIEW FV10i confocal microscope at 400× of original magnification.

the expression of DAXX in a dose- and time-dependent manner (Fig. 4B and C). Of significance, co-treatment of PGG and NAC obviously restrained JNK phosphorylation and DAXX suppression compared with the cells treated with PGG alone (Fig. 4D). In addition, NAC significantly blocked caspase-3 activation, PARP cleavage and Bcl-2 downregulation induced by PGG (Fig. 4D). Immunocytochemistry further confirmed that PGG repressed the expression of DAXX, which was reversed by NAC in K562 cells (Fig. 4E).

4. Discussion

In the current study, the underlying mechanism for a phenolic compound PGG-induced apoptosis in chronic myeloid leukemia (CML) K562 cells was examined. PGG significantly inhibited the viability of K562 and KBM-5 cells, but did not hurt normal peripheral blood lymphocytes.

PGG-mediated apoptosis was proved by apoptotic bodies, sub-G1 accumulation and DNA fragmentation, implying the apoptotic

feature of PGG in K562 cells. Apoptosis signaling is controlled by intrinsic mitochondria-mediated pathway and/or extrinsic receptor-mediated pathways [17] mediated by activation of caspase (cystein-aspartic protease) family protein(s) [18]. Here, PGG remarkably activated caspase-8 (extrinsic pathway) and -9 (intrinsic pathway) in a dose- and time-dependent manner, indicating both intrinsic and extrinsic pathways are involved in PGG-induced apoptosis in K562 cells. Additionally, PGG treatment significantly promoted caspase-3 activation and cleaved PARP, a substrate of caspase-3, in a time- and dose-dependent manner. Also, pretreatment of caspase inhibitors including z-VAD-fmk (pan caspase inhibitor), z-DEVD-fmk (caspase-3 inhibitor), z-IETD-fmk (caspase-8 inhibitor), and z-LEHD-fmk (caspase-9 inhibitor) disrupted the ability of PGG to induce PARP cleavage and caspase-3 activation in PGG-treated K562cells, suggesting PGG induced caspase-3-dependent apoptosis.

The Bcl-2 and IAP protein families play pivotal roles in apoptosis pathway [19]. In our study, down-regulation of anti-apoptotic Mcl-1_L, Bcl-2 (Bcl-2 family), and Survivin (IAP family) was observed in PGG treated K562 cells in a dose- and time-dependent manner. However, PGG did not affect the expression of Bcl-x_L (Bcl-2 family), c-IAP1 and c-IAP2 (IAP family) (data not shown). Interestingly, although recent studies reported that myeloid cell leukemia-1 (Mcl-1) has identified as a Bcr/Abl dependent survival factor in CML [20–22], CML KBM-5 showed weak expression of Mcl-x_L compared to other leukemic cells such as HL-60 and U937 cells.

ROS plays an essential role in a variety of normal biochemical functions and abnormal pathological processes, and excessive ROS production is sometimes associated with apoptosis induction [23,24] . ROS at the early stage of apoptosis induces the depolarization of the mitochondrial membrane, which eventually results in an increase in the level of other proapoptotic molecules in the cytosol [25]. There are evidences that cytotoxic ROS signaling is associated in part with activation of the apoptosis signal-regulating kinase 1 (ASK1)/mitogen-activated protein kinase (MAPK) signaling pathway [26]. Also, JNK/SAPK is an essential protein kinase in a diverse array of cellular functions including proliferation, differentiation and apoptosis [27]. Hence, flow cytometric analysis revealed that PGG significantly increased ROS production compared to untreated control. Conversely, NAC treatment clearly blocked PGG-mediated ROS generation in K562 cells indicating the important role of ROS signaling in PGG induced apoptosis in. Consistently, Bioplex assay and Western blotting showed a dramatic increase of JNK phosphorylation by PGG treatment in a dose- and time-dependent manner. PGG significantly attenuated apoptosis induction in the presence of JNK inhibitor, but not ERK and p38 MAPK inhibitors, implying the key role of JNK in PGG-induced apoptosis signaling pathway. DAXX is an upstream molecule of JNK in ROS-mediated apoptosis pathway [28,29]. PGG suppressed the expression of DAXX protein in K562 cells. Furthermore, a ROS scavenger NAC clearly blocked PGG-mediated ROS production, DAXX inhibition, JNK activation and apoptosis induction by Western blotting and immunofluorescence staining, demonstrating that PGG-induced apoptosis is regulated through the ROS/DAXX/JNK pathway in K562 cells.

In summary, PGG activated caspases (8,9,3) and cleaved PARP, increased sub G1 accumulation and suppressed survival genes such as Mcl-1_L, Bcl-2 and Survivin in CML K562 cells. Interestingly, PGG produced ROS and upregulated JNK and its upstream DAXX and their inhibitors blocked PGG induced apoptosis by Western blotting. Taken together, our findings suggest that PGG can be a potential chemotherapeutic agent or CML therapy by targeting the ROS/DAXX/JNK signaling pathway.

Acknowledgment

This work was supported by the National Research Foundation of Korea (NRF) grant funded by the Korea government [MEST] (No. 2012-0005755).

References

[1] S. Faderl, M. Talpaz, Z. Estrov, H.M. Kantarjian, Chronic myelogenous leukemia: biology and therapy, Ann. Intern. Med. 131 (1999) 207–219.
[2] C.L. Sawyers, Chronic myeloid leukemia, N. Engl. J. Med. 340 (1999) 1330–1340.
[3] J. Zhang, L. Li, S.H. Kim, A.E. Hagerman, J. Lu, Anti-cancer, anti-diabetic and other pharmacologic and biological activities of penta-galloyl-glucose, Pharm. Res. 26 (2009) 2066–2080.
[4] H. Hu, H.J. Lee, C. Jiang, J. Zhang, L. Wang, Y. Zhao, Q. Xiang, E.O. Lee, S.H. Kim, J. Lu, Penta-1,2,3,4,6-O-galloyl-beta-D-glucose induces p53 and inhibits STAT3 in prostate cancer cells in vitro and suppresses prostate xenograft tumor growth in vivo, Mol. Cancer Ther. 7 (2008) 2681–2691.
[5] J.E. Huh, E.O. Lee, M.S. Kim, K.S. Kang, C.H. Kim, B.C. Cha, Y.J. Surh, S.H. Kim, Penta-O-galloyl-beta-D-glucose suppresses tumor growth via inhibition of angiogenesis and stimulation of apoptosis: roles of cyclooxygenase-2 and mitogen-activated protein kinase pathways, Carcinogenesis 26 (2005) 1436–1445.
[6] W.J. Chen, C.Y. Chang, J.K. Lin, Induction of G1 phase arrest in MCF human breast cancer cells by pentagalloylglucose through the down-regulation of CDK4 and CDK2 activities and up-regulation of the CDK inhibitors p27(Kip) and p21(Cip), Biochem. Pharmacol. 65 (2003) 1777–1785.
[7] L.L. Ho, W.J. Chen, S.Y. Lin-Shiau, J.K. Lin, Penta-O-galloyl-beta-D-glucose inhibits the invasion of mouse melanoma by suppressing metalloproteinase-9 through down-regulation of activator protein-1, Eur. J. Pharmacol. 453 (2002) 149–158.
[8] G.S. Oh, H.O. Pae, H. Oh, S.G. Hong, I.K. Kim, K.Y. Chai, Y.G. Yun, T.O. Kwon, H.T. Chung, In vitro anti-proliferative effect of 1,2,3,4,6-penta-O-galloyl-beta-D-glucose on human hepatocellular carcinoma cell line, SK-HEP-1 cells, Cancer Lett. 174 (2001) 17–24.
[9] K. Miyamoto, N. Kishi, R. Koshiura, T. Yoshida, T. Hatano, T. Okuda, Relationship between the structures and the antitumor activities of tannins, Chem. Pharm. Bull. (Tokyo) 35 (1987) 814–822.
[10] X. Yang, R. Khosravi-Far, H.Y. Chang, D. Baltimore, Daxx, a novel Fas-binding protein that activates JNK and apoptosis, Cell 89 (1997) 1067–1076.
[11] Y. Chai, H.J. Lee, A.A. Shaik, K. Nkhata, C. Xing, J. Zhang, S.J. Jeong, S.H. Kim, J. Lu, Penta-O-galloyl-beta-D-glucose induces G1 arrest and DNA replicative S-phase arrest independently of P21 cyclin-dependent kinase inhibitor 1A, P27 cyclin-dependent kinase inhibitor 1B and P53 in human breast cancer cells and is orally active against triple-negative xenograft growth, Breast Cancer Res. 12 (2010) R67.
[12] H.J. Seo, J.E. Huh, J.H. Han, S.J. Jeong, J. Jang, E.O. Lee, H.J. Lee, K.S. Ahn, S.H. Kim, Polygoni rhizoma inhibits inflammatory response through inactivation of nuclear factor-kappaB and mitogen activated protein kinase signaling pathways in RAW264.7 mouse macrophage cells., Phytother. Res. 26 (2) (2011) 239–245.
[13] J.H. Kim, S.J. Jeong, T.R. Kwon, S.M. Yun, J.H. Jung, M. Kim, H.J. Lee, M.H. Lee, S.G. Ko, C.Y. Chen, S.H. Kim, Cryptotanshinone enhances TNF-alpha-induced apoptosis in chronic myeloid leukemia KBM-5 cells, Apoptosis 16 (2011) 696–707.
[14] S. Kumar, Mechanisms mediating caspase activation in cell death, Cell Death Differ. 6 (1999) 1060–1066.
[15] S.W. Ryter, H.P. Kim, A. Hoetzel, J.W. Park, K. Nakahira, X. Wang, A.M. Choi, Mechanisms of cell death in oxidative stress, Antioxid. Redox. Signal 9 (2007) 49–89.
[16] A.F. Khelifi, M.S. D'Alcontres, P. Salomoni, Daxx is required for stress-induced cell death and JNK activation, Cell Death Differ. 12 (2005) 724–733.
[17] S. Fulda, Evasion of apoptosis as a cellular stress response in cancer, Int. J. Cell Biol. 2010 (2010) 370835.
[18] E.A. Slee, C. Adrain, S.J. Martin, Serial killers: ordering caspase activation events in apoptosis, Cell Death Differ. 6 (1999) 1067–1074.
[19] B. Antonsson, Mitochondria and the Bcl-2 family proteins in apoptosis signaling pathways, Mol. Cell Biochem. 256–257 (2004) 141–155.
[20] Q.F. Li, J. Yan, K. Zhang, Y.F. Yang, F.J. Xiao, C.T. Wu, H. Wang, L.S. Wang, Bortezomib and sphingosine kinase inhibitor interact synergistically to induces apoptosis in BCR/ABl+ cells sensitive and resistant to STI571 through down-regulation Mcl-1, Biochem. Biophys. Res. Commun. 405 (2011) 31–36.
[21] G. Dasmahapatra, N. Yerram, Y. Dai, P. Dent, S. Grant, Synergistic interactions between vorinostat and sorafenib in chronic myelogenous leukemia cells involve Mcl-1 and p21CIP1 down-regulation, Clin. Cancer Res. 13 (2007) 4280–4290.
[22] Q.F. Li, W.R. Huang, H.F. Duan, H. Wang, C.T. Wu, L.S. Wang, Sphingosine kinase-1 mediates BCR/ABL-induced upregulation of Mcl-1 in chronic myeloid leukemia cells, Oncogene 26 (2007) 7904–7908.

[23] F. Thayyullathil, S. Chathoth, A. Hago, M. Patel, S. Galadari, Rapid reactive oxygen species (ROS) generation induced by curcumin leads to caspase-dependent and -independent apoptosis in L929 cells, Free Radic. Biol. Med. 45 (2008) 1403–1412.

[24] M.L. Circu, T.Y. Aw, Reactive oxygen species, cellular redox systems, and apoptosis, Free Radic. Biol. Med. 48 (2010) 749–762.

[25] C.M. Shih, W.C. Ko, J.S. Wu, Y.H. Wei, L.F. Wang, E.E. Chang, T.Y. Lo, H.H. Cheng, C.T. Chen, Mediating of caspase-independent apoptosis by cadmium through the mitochondria-ROS pathway in MRC-5 fibroblasts, J. Cell Biochem. 91 (2004) 384–397.

[26] A. Matsuzawa, H. Ichijo, Redox control of cell fate by MAP kinase: physiological roles of ASK1-MAP kinase pathway in stress signaling, Biochim. Biophys. Acta 1780 (2008) 1325–1336.

[27] M. Karin, E. Gallagher, From JNK to pay dirt: jun kinases, their biochemistry, physiology and clinical importance, IUBMB Life 57 (2005) 283–295.

[28] C. Li, J. Zhou, X. Wu, Y. Tian, J. Deng, W. Liu, Induction of myelogenous leukemia cells with histone deacetylase inhibitors through down-regulating the Daxx protein expression, J. Huazhong Univ. Sci. Technolog. Med. Sci. 29 (2009) 546–550.

[29] R. Zobalova, E. Swettenham, J. Chladova, L.F. Dong, J. Neuzil, Daxx inhibits stress-induced apoptosis in cardiac myocytes, Redox. Rep. 13 (2008) 263–270.